Supplement to "Coral calcifying fluid aragonite saturation states derived from Raman spectroscopy": additional measurement details

Raman peak widths are known to be sensitive to instrument configuration (Nasdala et al., 2001; Wang et al., 2012; Váczi, 2014). Measured peak width is generally considered a convolution of a Gaussian curve that reflects instrument noise, and the true Lorentzian sample peak (Verma et al., 1995). The width of the instrumental peak depends on the spectral resolution (Nasdala et al., 2001). If spectral resolution is too low, the instrumental peak can partially or completely obscure variations of the sample peak width. Measurements of the abiogenic aragonites (Table S1) conducted on the WITec instrument with 600 mm^{-1} grating and a spectral resolution of 3 cm^{-1} produced wider peaks and noisier results, compared to the measurements conducted with 1200 mm^{-1} grating at 1.3 cm^{-1} resolution (Fig. S1). The effect of spectral resolution on measured peak width can be accounted for using the formula of Nasdala et al. (2001) (equation 3 in main text). Following this correction brings the measurements conducted on the WITec and the Horiba instruments close to a 1:1 line (Table S2; Fig. S2). This is critical because it suggests that measurements conducted in other laboratories should be able to use the FWHM-Ω_{Ar} calibration presented here, if spectral resolution is known and the true sample peak widths are calculated. Indeed, the calibration remains effectively constant over time and thus daily instrument calibration using abiogenic samples is not necessarily required for detecting Ω_{Ar} changes > ~2 units (Fig. S3). However, it is important to recognize that the Nasdala et al. (2001) formula is only valid when the true peak width exceeds twice the spectral resolution, meaning that for a true peak width of 2.9 cm^{-1} (Ω_{Ar} of approximately 10), a spectral resolution of 1.45 cm^{-1} or better is required. To achieve this resolution on the WITec instrument required using a 1200 mm^{-1} grating, which allowed a spectral range of only 750 cm^{-1}. This relatively small spectral range made it impossible to capture both the 1085 cm^{-1} ν_1 peak and the aragonite lattice modes in the 100-250 cm^{-1} range. We found the optimal configuration was to place the spectral center at 830 cm^{-1}, which captures both the ν_1 FWHM to calculate Ω_{Ar}, and the ~705 cm^{-1} ν_4 peak to confirm the presence of aragonite.

The precision of peak width measurements depends not only on the spectral resolution, but also on integration time. Relatively long (short) integration times will produce high (low) signal-noise ratios. We repeatedly (n=10) analysed the same spot on the same aragonite grain (from experiment f06) using integration times ranging from 0.05 s to 10 s. The standard deviation (σ) of ν_1 FWHM decreased with longer integration times (Fig. S4). At 0.05 s integration time, the σ of ν_1 FWHM was 0.2 cm^{-1}, which covers more than half of the range of the calibration between Ω_{Ar} 10 and 30. Integration time of at least 0.5 s was required to reduce σ below 0.05 cm^{-1} ($\pm$ 1 Ω_{Ar} unit). The improvement in precision decreases beyond 1 s integration time, and thus we found that integration times between 0.5 and 1 s provided the best compromise between precision and analysis time. Calibration between ν_1 FWHM and Ω_{Ar} was practically identical using integration times of 1 s or 5 s, but the slope became slightly shallower with integration time of 0.1 s, likely due to decreasing precision and measurement noise (Fig. S5).

In the main text, we fit ν_1 FWHM as a function of Ω_{Ar} because Ω_{Ar} is likely the independent variable and ν_1 FWHM the dependent variable. The calibration could alternatively be carried out with Ω_{Ar} as a function of ν_1 FWHM in order to minimise errors in Ω_{Ar} (Fig. S6). However, the two calibration techniques are nearly identical, and have little influence on Ω_{Ar} values derived from ν_1 FWHM measurements. For example, applying this alternate calibration to our JCp-1 measurements gives a mean derived Ω_{Ar} of 12.23 compared to 12.30 with the calibration in Table 2.

References

DeCarlo, T. M., Gaetani, G. A., Holcomb, M., and Cohen, A. L.: Experimental determination of factors controlling U/Ca of aragonite precipitated from seawater: implications for interpreting coral skeleton, Geochimica et cosmochimica acta, 162, 151–165, doi:doi:10.1016/j.gca.2015.04.016, 2015.

Holcomb, M., DeCarlo, T., Gaetani, G., and McCulloch, M.: Factors affecting B/Ca ratios in synthetic aragonite, Chemical Geology, 437, 67–76, doi:10.1016/j.chemgeo.2016.05.007, 2016.

Nasdala, L., Wenzel, M., Vavra, G., Irmer, G., Wenzel, T., and Kober, B.: Metamictisation of natural zircon: accumulation versus thermal annealing of radioactivity-induced damage, Contributions to Mineralogy and Petrology, 141, 125–144, doi:10.1007/s004100000235, 2001.

Váczi, T.: A New, Simple Approximation for the Deconvolution of Instrumental Broadening in Spectroscopic Band Profiles, Applied Spectroscopy, 68, 1274–1278, doi:10.1366/13-07275, 2014.

Verma, P., Abbi, S. C., and Jain, K. P.: Raman-scattering probe of anharmonic effects in GaAs, Physical Review B, 51, 16 660–16 667, doi:10.1103/PhysRevB.51.16660, 1995.

Wang, D., Hamm, L. M., Bodnar, R. J., and Dove, P. M.: Raman spectroscopic characterization of the magnesium content in amorphous calcium carbonates, Journal of Raman Spectroscopy, 43, 543–548, 2012.

Table S1. Summary of fluid conditions and precipitate Mg/Ca for the abiogenic aragonites analysed in this study

ID	T	Ω_{Ar}	G	pH	$[CO_3^{2-}]$	Mg/Ca	$K_D^{\text{Mg/Ca}}$
	(°C)		(mmol m^{-2} hr^{-1})	(total scale)	(μmol kg^{-1})	(mmol mol^{-1})	(x10^{-3})
h02	20	29 (4)	3.4	8.88 (0.01)	2060 (90)	9.15	1.68 (0.02)
h08	20	21 (4)	2.2	8.20 (0.01)	1600 (90)	6.73	1.17 (0.01)
f01	25.5	16 (4)	4.1	8.62 (0.02)	1310 (70)	7.52	1.01 (0.01)
f02	25.5	19 (3)	5.6	8.48 (0.02)	1400 (100)	7.53	1.22 (0.01)
f03	25.5	30 (4)	13	8.96 (0.02)	2100 (100)	9.58	1.63 (0.02)
f04	25.5	19 (3)	5.6	8.16 (0.01)	1380 (70)	7.18	1.12 (0.01)
f05	25.5	34 (3)	16	9.03 (0.01)	2560 (80)	11.3	1.76 (0.02)
f06	25.5	11 (1)	2	8.38 (0.01)	860 (60)	4.93	0.77 (0.01)
f08	25.5	12 (4)	2.4	7.90 (0.07)	600 (200)	2.56	-
g01	25.5	21 (4)	6.7	8.80 (0.02)	1600 (100)	8.35	1.41 (0.01)
g02	25.5	25 (1)	8.2	8.40 (0.04)	1600 (100)	7.18	1.30 (0.02)
g03	25.5	17 (3)	4.6	8.43 (0.01)	1230 (80)	6.14	1.06 (0.01)
g04	25.5	25 (3)	9.1	8.48 (0.01)	1720 (60)	7.67	1.39 (0.01)
g05	25.5	18 (2)	5	8.02 (0.02)	1320 (70)	6.55	1.10 (0.02)
g07	25.5	24 (3)	8.4	8.00 (0.01)	1700 (200)	7.42	1.31 (0.01)
g08	25.5	26 (4)	9.7	8.49 (0.02)	1900 (100)	8.23	1.36 (0.02)
g09	25.5	23 (5)	7.8	7.78 (0.02)	1700 (200)	6.84	1.10 (0.02)
g10	25.5	18 (3)	5	8.06 (0.04)	1500 (100)	7.37	1.09 (0.02)
g11	25.5	17 (2)	4.6	7.79 (0.02)	1290 (70)	6.26	1.04 (0.01)
g13	25.5	10 (3)	1.7	7.89 (0.02)	600 (100)	2.46	-
h01	25.5	21 (4)	6.7	8.86 (0.01)	1690 (80)	9.28	1.50 (0.01)
h09	25.5	14 (3)	3.2	7.89 (0.03)	1100 (100)	5.56	0.85 (0.01)
h10	25.5	21 (4)	6.7	7.78 (0.03)	1600 (100)	7.9	1.30 (0.03)
h13	25.5	28 (12)	11	9.32 (0.02)	1900 (500)	11.1	1.81 (0.02)
h03	33	17 (3)	18	8.69 (0.03)	1300 (100)	7.29	1.23 (0.02)
h07	33	15 (1)	14	8.13 (0.03)	1070 (40)	6.19	1.13 (0.01)
h05	40	15 (2)	45	8.67 (0.01)	1110 (40)	7.08	1.23 (0.01)
h06	40	12 (2)	24	8.12 (0.04)	850 (60)	5.64	1.00 (0.01)

Notes: Carbonate chemistry and temperature data were published in DeCarlo et al. (2015) and Mg/Ca data are from Holcomb et al. (2016); numbers in parentheses indicate 1 standard deviation during the course of aragonite precipitation. $K_D^{\text{Mg/Ca}}$ was calculated following DeCarlo et al. (2015).

Table S2. Summary of Raman peak characteristics

ID	Horiba measured ν_1 height	Horiba measured ν_1 position (cm^{-1})	Horiba measured ν_1 FWHM (cm^{-1})	Horiba TRUE ν_1 FWHM (cm^{-1})	WITec measured ν_1 FWHM (cm^{-1})	WITec TRUE ν_1 FWHM (cm^{-1})
h02	1.1 (0.2)	-	3.97 (0.04)	3.58 (0.05)	-	-
h08	2.1 (0.3)	1085.15 (0.11)	3.89 (0.08)	3.50 (0.08)	-	-
f01	1.6 (0.1)	1085.38 (0.01)	3.57 (0.14)	3.14 (0.16)	-	-
f02	1.4 (0.3)	1085.36 (0.03)	3.61 (0.04)	3.19 (0.04)	3.75 (0.02)	3.27 (0.02)
f03	1.5 (0.3)	1085.34 (0.01)	4.06 (0.04)	3.69 (0.04)	4.05 (0.02)	3.61 (0.02)
f04	2.0 (0.1)	1085.40 (0.02)	3.73 (0.02)	3.32 (0.03)	-	-
f05	0.6 (0.1)	-	4.08 (0.03)	3.70 (0.03)	-	-
f06	3.4 (0.3)	1085.34 (0.03)	3.35 (0.03)	2.89 (0.03)	3.45 (0.01)	2.92 (0.01)
f08	1.0 (0.1)	1085.07 (0.04)	3.45 (0.02)	3.00 (0.02)	-	-
g01	1.1 (0.2)	1085.31 (0.01)	3.94 (0.03)	3.56 (0.03)	-	-
g02	2.6	-	3.95	3.57	-	-
g03	2.2	1085.4	3.7	3.28	-	-
g04	1.4 (0.1)	1085.36 (0.02)	3.96 (0.03)	3.58 (0.03)	-	-
g05	2.2 (0.8)	1085.35 (0.01)	3.56 (0.10)	3.13 (0.11)	-	-
g07	1.5 (0.1)	-	3.88 (0.02)	3.49 (0.03)	3.91 (0.02)	3.45 (0.02)
g08	1.5 (0.1)	-	4.01 (0.02)	3.64 (0.02)	-	-
g09	1.4 (0.3)	-	3.63 (0.03)	3.21 (0.04)	-	-
g10	1.4 (0.1)	1085.32 (0.01)	3.52 (0.06)	3.08 (0.07)	-	-
g11	1.5 (0.1)	1085.41 (0.02)	3.44 (0.06)	2.99 (0.06)	-	-
g13	1.6 (0.2)	1085.25 (0.03)	3.32 (0.02)	2.86 (0.02)	3.46 (0.01)	2.93 (0.01)
h01	1.2 (0.1)	1085.31 (0.04)	3.70 (0.06)	3.28 (0.07)	-	-
h09	1.9 (0.2)	1085.46 (0.03)	3.37 (0.03)	2.92 (0.03)	3.52 (0.01)	3.00 (0.01)
h10	2.0 (0.4)	1085.32 (0.03)	3.79 (0.05)	3.39 (0.06)	-	-
h13	2.9 (0.3)	1085.33 (0.01)	4.00 (0.04)	3.63 (0.04)	-	-
h03	1.9 (0.2)	1085.38 (0.02)	3.56 (0.05)	3.13 (0.05)	-	-
h07	1.7 (0.3)	1085.38 (0.01)	3.63 (0.08)	3.20 (0.09)	-	-
h05	1.5 (0.1)	1085.40 (0.03)	3.52 (0.06)	3.09 (0.07)	-	-
h06	3.5	1085.41	3.37	2.91		

Notes: Numbers in parentheses indicate 1 standard error of the mean of replicate Raman spectra. Where no parentheses are displayed, only 1 spectrum was collected. Dashes in the position column indicate spectra collected on a different day when the wavenumber calibration drifted by 2 cm^{-1} and were thus excluded.

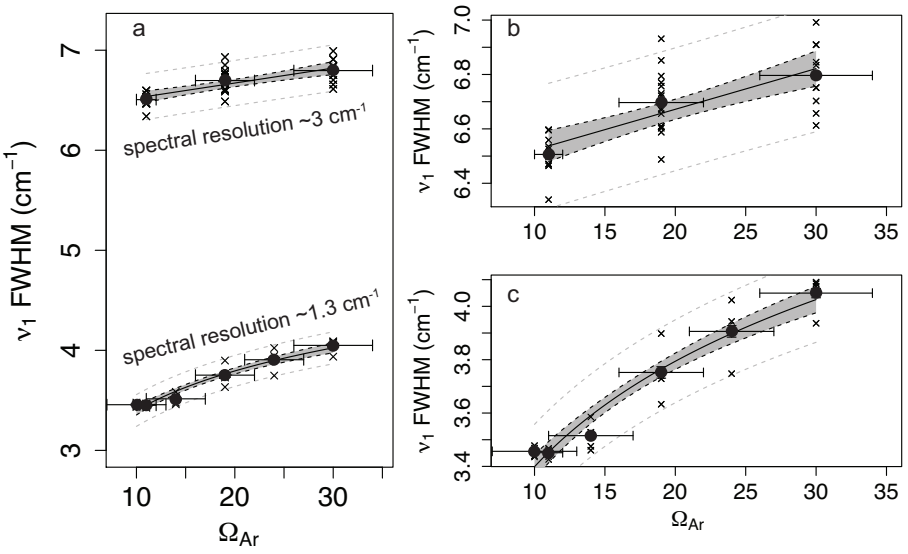

Figure S1. Effect of spectral resolution on FWHM measurements. (a) ν_1 FWHM of the same aragonites measured on the WITec instrument with 3 cm^{-1} and 1.3 cm^{-1} resolution. (b-c) Same as panel (a), but with y-axes scaled for measurements made at 3 cm^{-1} and 1.3 cm^{-1} resolution, respectively.

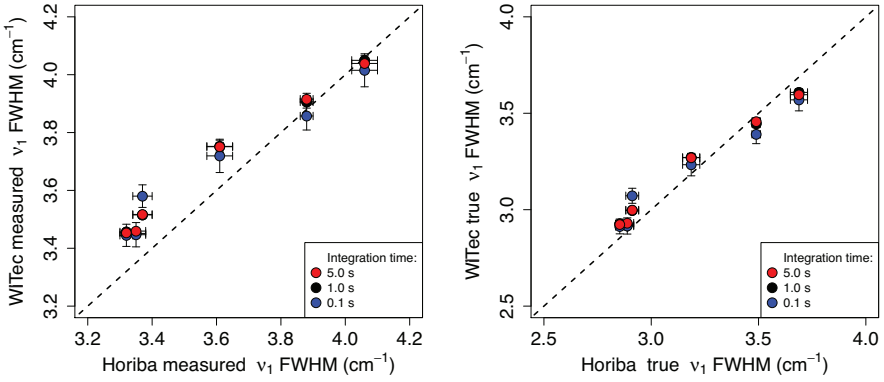

Figure S2. Correction of ν_1 FWHM for spectral resolution. Scatter plots of measured (left) and true (right) ν_1 FWHM from the Horiba and WITec instruments. Colours show measurements on the WITec instrument conducted with various integration times.

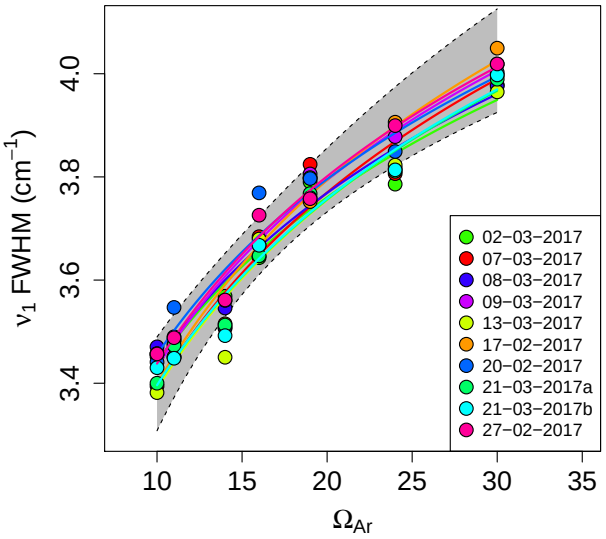

Figure S3. Calibrations between measured ν_1 FWHM and Ω_{Ar} determined on multiple days with the WITec instrument. The grey error bound shows the confidence interval for the calibration reported in Table 2. Note that horizontal error bars have been excluded for clarity.

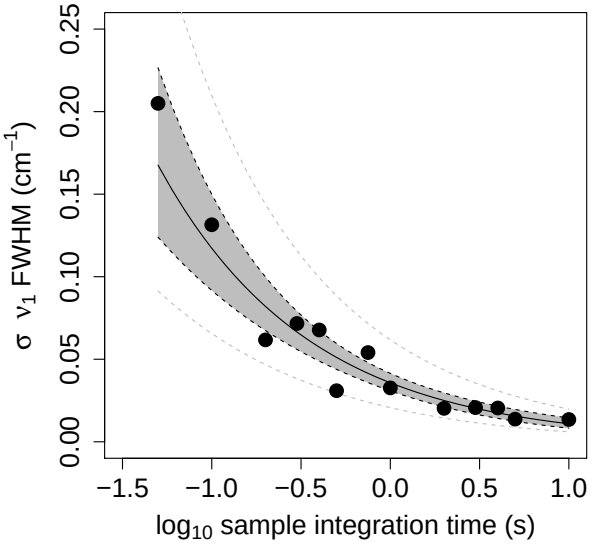

Figure S4. Effect of integration time on precision of ν_1 FWHM measurements. Each point represents 1 σ of 10 measurements made on the same spot. Grey shading represents the standard error of the curve, and the dashed grey lines represent the standard error of prediction.

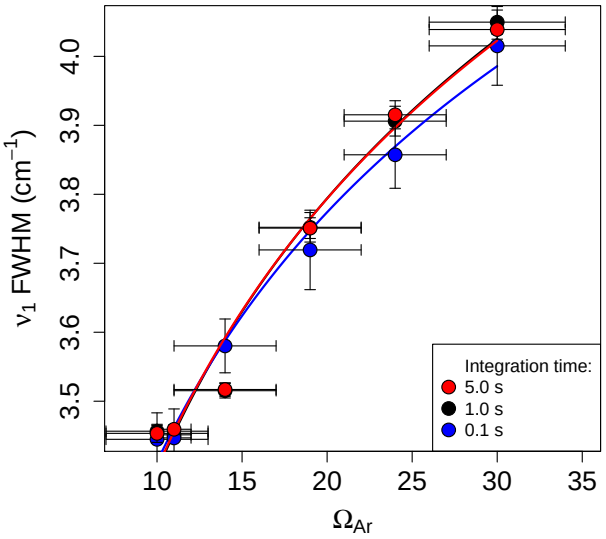

Figure S5. Effect of integration time on the calibration between measured ν_1 FWHM and Ω_{Ar}. Red, black, and blue points and lines show calibrations conducted using 5 s, 1 s, and 0.1 s integration times, respectively.

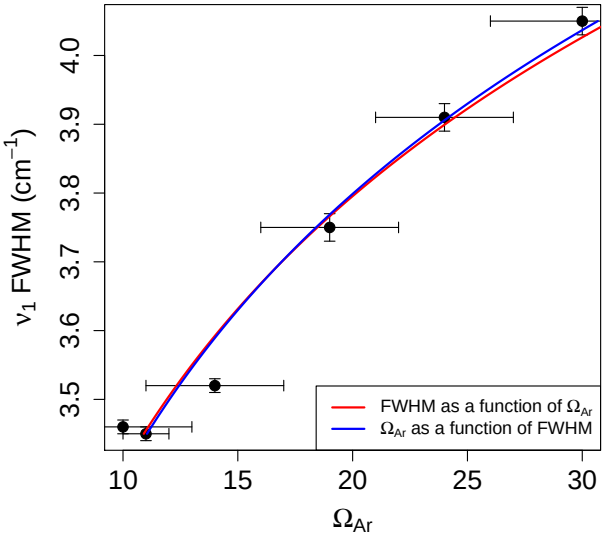

Figure S6. Comparison of fitting ν_1 FWHM as a function of Ω_{Ar} (red), and fitting Ω_{Ar} as a function of ν_1 FWHM (blue). The latter calibration equation is $ln(\Omega_{Ar})$ = 1.703 * ν_1 FWHM - 3.472.